COBEM 2023 27TH INTERNATIONAL CONGRESS OF MECHANICAL ENGENEERING

ABCM Brazilian Society of Mechanical Sciences and Engineering
27th ABCM International Congress of Mechanical Engineering
December 04-08, 2023, Florianópolis-SC, Brazil

# COB-2023-2295
# OPTIMIZATION OF CEMENT PASTE FORMULATION FOR RHEOMETRIC EXPERIMENTS

**Patricia Almeida**
**Eliana Paola Marín Castaño**
**Paulo R. de Souza Mendes**
Department of Mechanical Engineering, Pontifícia Universidade Católica do Rio de Janeiro, Rua Marquês de São Vicente 225, Rio de Janeiro, RJ 22453-900, Brazil
patricialmeida2998@gmail.com, epmarinc1053@gmail.com, pmendes@puc-rio.br

**Elias da Conceição Rodrigues**
School of Applied Mathematics (FGV-EMAp) – Getúlio Vargas Foundation - Praia de Botafogo, 190 - 5º Andar - Botafogo, Rio de Janeiro - RJ, 22250-900) elias.rodrigues@fgv.br

***Abstract.*** *This work optimizes and controls paste preparation, guaranteeing no sedimentation or water separation. We varied the concentration of four additives and measured the percentage of free water and apparent yield stress. After testing 30 different formulations, we decided on the best composition of additives to obtain a paste with zero percentage of separated water, minimum sedimentation during 24 h, and high apparent yield stress. Finally, the hydration process of fresh cement pastes was characterized using calorimetry, rheology, and cryo-microscopy (cryo-SEM) techniques.*

***Keywords:*** *cement paste, rheology, cryo-SEM, hydration process, isotherm calorimetric curves.*

## 1. INTRODUCTION

Cement has many applications, depending on its type and composition. The most common request is in structures and buildings. However, there are other essential applications, including in the oil and gas industry, especially in production drilling and the completion of wells (Mangadlao *et al.* (2015)). The goal of well cementing is to provide zonal isolation of the wellbore, limiting gas, oil and water from moving one area to another in the well. Incomplete isolation or a frail seal may cause oil spills or reduce the producing potential of the well (Nelson (1990)).

The design of an optimal cement slurry depends on the characteristics of well cementing, such as geometry, formation integrity, drilling mud characteristics, and mixing conditions. Over the last few decades, different types of chemical admixtures (defoamers, retarders, dispersants, fluid loss, etc.) have been developed to improve the flow properties of cement-based products depending on the wellbore characteristics needed. The properties of cement-based systems at an early age and when they are hardened highly depend on the type and quantity of chemical additives. The chemical admixture selection is usually based on an experimental procedure using the mini-slump and other simple rheological tests (Shahriar (2011)).

Failure in cementing operations has caused historical accidents and production stops with very high costs. It is one of the reasons for an advance in the study of well cementing (Mangadlao *et al.* (2015)). It is well know that the complexity of cement is due to the condition of hydration by constantly changing its structure and its time-dependent rheological behavior (de Miranda *et al.* (2023); Rodrigues and de Souza Mendes (2019)). These conditions made this material interesting for its study and advancement. Due to these conditions, there are many difficulties that arise during the characterization of rheology and microstructure. Hence, the number of strictness studies is minimal.

The early-stage microstructure characterization of fresh cementitious materials is demanding. Conventional electron microscopy (SEM) cannot scan fresh paste in a hydrous or liquid state (Ylmén *et al.* (2009); Sun *et al.* (2022)). Studies have focused more on the solid fraction by using a destructive method. Further investigation is required to examine the microstructural properties of cement paste, such as through in-situ testing. The current in-situ method implies replacing the liquid fraction in the fresh paste with various organic solvents to stop the activation process (Zingg *et al.* (2008)). Then, the solid-filtered residues are collected and visualized through SEM. However, Zingg *et al.* (2008) reported that the original cement paste's pores are modified by solvent replacement. Otherwise, the cryogenic SEM (cryo-SEM) includes a rapid freezing process, avoiding ice crystallization, and a sublimation step, enabling the visualization of hydrating and highly moist samples. These conditions allow us to preserve the nature of microstructures well ( Sun *et al.* (2022); Talevi *et al.* (2016); Fylak *et al.* (2006)).

Cement formulation, an experimental protocol to find an optimal cement past for rheology testing, the complexity

of cement due to the hydration, the constantly changing chemical structure, and its time-dependent rheological behavior made this cementitious material challenging for study. After testing different combinations of formulations for controlled parameters such as $\%$ free water and empirical yield stress value, we find a formulation with optimal characteristics for rheological testing. We analyzed this chosen formulation using calorimetry, rheology, and cryo-SEM to understand the early hydration stage. The induction stage of the isotherm calorimetric curve is the best time to evaluate the rheology properties and obtain good repetitive results. Additionally, we correlated the cryo-SEM micrograph results with rheology and calorimetry. We observed particles suspended in a network that continuously increases and consolidates due to the generation of hydration products.

## 2. EXPERIMENTAL WORK

### 2.1 Material

The constituents employed included deionized water, cement Portland class G, a special cement for oil wells from Holcim, fluid loss, defoamer, and retarder additives from Kuraray. We ensured the water-to-cement ratio (W/C) remained at $44\%$ for all experiments.

### 2.2 Methodology

#### 2.2.1 Paste preparation

Initially, the cement powder and solid additives, namely the retarder and fluid loss agents, were precisely weighed. Subsequently, the liquid components, comprising water and defoamer, were also accurately measured in another container. Quantities were calculated for a volume of 600 ml of cement slurry. We used a stainless steel container with high-speed shear mixer from Chandler Engineering, USA, adhering to the API-10B procedure outlined by the American Petroleum Institute (2013a). A measured quantity of cement powder was uniformly introduced into the container at a speed of 4000 rpm for 15 s. Subsequently, the mixing speed was elevated to 1200 rpm and sustained for 35 seconds. The resulting paste achieved a final density of 2.52 g/cm$^3$. This paste was transferred for a consistometer from Chandler Engineering, USA, during 20 min at 27 °C.

#### 2.2.2 Measurement of controlled parameters: $\%$ free water and empirical yield stress

Cement paste, composed of various components with distinct densities, is susceptible to several instability phenomena. Two commonly observed occurrences in this material are blending, characterized by the separation of free water, and sedimentation, involving the precipitation of solid particles (Peng *et al.* (2017)). To investigate the blending phenomenon, we employed the free water test, also known as the Free fluid test, specified in ISO 10426-1:2009 (ISO *et al.*). In this test, we introduced 35 ml of the freshly prepared paste into a test tube and allowed it to stand for one hour. Subsequently, we visually assessed the quantity (volume) of free fluid present and calculated the ratio between this volume and the total volume using Equation 1.

$$\varphi = \frac{V_{FF} \cdot \rho}{m_S} \cdot 100, \tag{1}$$

Where $V_{FF}$ is the volume of free fluid (supernatant fluid) collected (ml), $\rho$ is the specific gravity of the slurry, and $m_S$ is the initially recorded (starting) mass of the slurry (g).

The spreading test was employed as a predictive technique to ascertain the apparent yield stress of cement paste. This method has found extensive application in numerous industrial contexts, owing to its convenience and rapidity in evaluating the apparent yield stress of suspensions and pasty substances (Roussel and Coussot (2005)). It is important to emphasize that the slump test provides an apparent stress value, which signifies the fluid resistance expected under specific conditions. In our study, we utilized this test as a control parameter, aiding us in determining the optimal paste formulation.

The slump-spread test entails rapidly releasing a paste volume onto a horizontal surface (Baudez *et al.* (2002); Roussel *et al.* (2005)). The analysis of the resulting flow is determined by the ratio between the height (h) and the radius (R) of the sample. When h>>R, it is referred to as the slump test, whereas when h<<R, it is recognized as the spread test. In our study, the height (h) was smaller than the radius (R), categorizing it as a spreading test. Existing literature highlights that surface tension can significantly influence the yield stress value when relatively low. However, considering that our experiments' spread radius (R) was below the 35 cm threshold established by Roussel *et al.* (2005) for a limited spread ratio, we deemed the surface tension effects negligible compared to the yield value effect. Thus, we proceeded with the following equation:

$$\tau_0 = \frac{225 \cdot \rho \cdot g \cdot V^2}{128\pi^2 \cdot R^5}, \tag{2}$$

Where $\tau_0$ is the apparent yield stress, $g$ is the gravity, $V$ is the volume of the slurry ($m^3$), and $R$ is the radius.

#### 2.2.3 Calorimetry heat flow test

We employed an isothermal calorimeter to assess the impact of particular additives on the generation of heat reactions during cementing. Four distinct samples were allocated to separate channels and maintained at a temperature of 23 °C. These experiments were conducted following ASTM C1702 Method B (external mixing) utilizing the I-CAL 4000 HPC isothermal conduction calorimeter manufactured by Calmetrix.

#### 2.2.4 Rheology characterization

The rheological characterization of the pastes were assessed using a TA Instruments Discovery hybrid rheometer equipped with a 60 mm diameter crosshatched Peltier plate. A new paste was prepared for each test to ensure accurate measurements and eliminate any influence from prior shear history. The freshly prepared paste was carefully placed onto the plate geometry and allowed to rest undisturbed for 20 minutes, ensuring the sample reached a homogeneous temperature of 25 °C. Subsequently, a constant shear rate curve was performed at a rate of $\dot{\gamma} = 1s^{-1}$ until the initial signs of an exponential increase in viscosity were observed.

#### 2.2.5 Microscopy characterization

The microstructures of cement paste at various ages (30 min, 1 h, and 3 h) were examined using Cryo-SEM, employing the TESCAN CLARA field-free Ultra-High Resolution (UHR) electron microscope. The specimen was rapidly frozen in liquid nitrogen (-210 °C) under vacuum conditions to preserve the sample's integrity and prevent ice crystallization (Talevi *et al.* (2016)), suspending the cementing reactions (Sun *et al.* (2022)). Subsequently, the vitrified sample was transferred under vacuum to a cryo chamber from Quorum Technologies Ltd., East Sussex, U.K., maintained at -140 °C. The frozen sample was then fractured using a cooled knife and subjected to a 5-minute etching process at -60 °C in the preparation chamber to sublimate the water content. A thin layer of conductive metal (Pt) was sputter-coated onto the sample. SEM observations were conducted under vacuum conditions at -140 °C, utilizing an accelerated voltage of 5 kV.

## 3. RESULTS AND DISCUSSION

As mentioned earlier, one of our primary objectives was to optimize the formulation of cement paste, aiming to achieve desirable rheological properties. This approach was motivated by the inherent limitations of rheometers when applied to materials that exhibit instability, such as water separation and sedimentation. The following section presents a detailed account of the materials utilized and the methodology applied to find the optimal paste.

### 3.1 Finding the optimal cement paste

We conducted extensive testing, evaluating nearly 30 different formulations, to identify the optimal cement paste composition that exhibited stability with zero percent free water and a high empirical yield stress. The results were graphically represented, plotting the percentage of free water (Fig. 1a), the apparent yield stress (Fig. 1b), and the quantities of the components as percentages (Fig. 1c) against the number of formulations tested. We determined that the optimal values for these parameters were achieved by increasing the quantity of the Fluid Loss additive to 2 percent and eliminating the dispersant additive. The apparent yield stress was maintained at a close and constant value of 8 Pa for the last three tests. Table 1 displays the weight-proportional additives composition utilized for this optimal formulation.

Table 1: Composition of the optimal cement paste (W/C 44 %).

| **Composites** | **class** | **wt**% |
|---|---|---|
| Fluid loss | Kuraray | 2 |
| Defoamer | Basupur DF 5 | 0.2 |
| Retarder | CemR-10 | 0.05 |

After choosing the best formulation, we continued with the characterization of the paste by calorimetry to observe the effect of each additive in the hydration process. Isothermal calorimetry is a widely employed technique for studying the kinetics of cement hydration (see Fig. 2). The calorimetry curve typically exhibits four distinct stages for ordinary Portland cement. Firstly, intense heat is rapidly released upon contact between the cement and water. Subsequently, the heat flow rate reaches its lowest point during an induction phase. After this resting period, the third stage is characterized by an increase in the heat generation rate, which can be attributed to the crystallization and precipitation of hydration products involving nucleation and growth processes. Finally, the heat evolution rate decreases after reaching the maximum

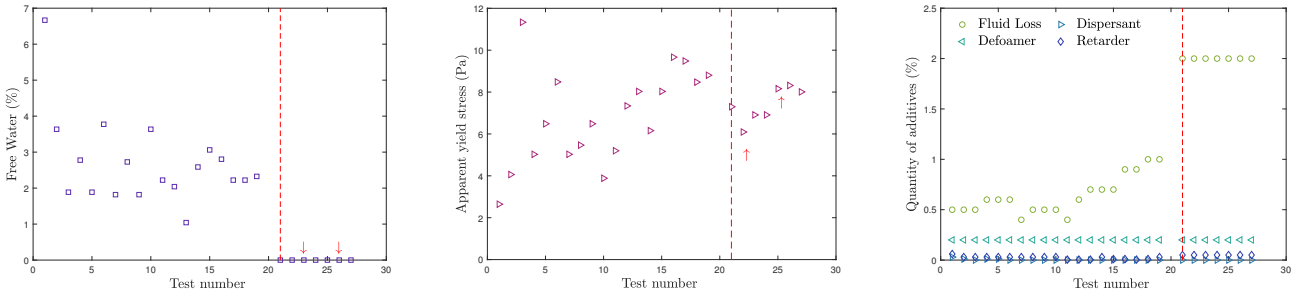


(a) Percentage of Free water separeted after 24 h of rest.

(b) Empirical yield stress by spreading test.

(c) Quantity of additives for each formulation tested.

Figure 1: Experimental procedure to achieve the optimal cement paste ( water/cement (W/C of 44%). The discontinuous line marks the number of formulations we had to test for an excellent answer to control parameters. The formulation with the highest quantity of Fluid loss additive (2%) was the optimal cement paste because it zeroed out the Free Water quantity (more stable paste) and had the highest and equal value of empirical yield stress for three consecutive tests.

peak, which means the diffusion-controlled hydration process due to the complete coverage of clinkers by hydration products.

We conducted an isothermal calorimetry curve to isolate the role of each additive in the hydration process.Figure 2 shows four curves with different mixtures of cement and additives. We observed that adding retarder and defoamer dislocates the curves to the right, increasing the primary hydration time. The more notable change is that when a Fluid Loss additive was added, the heat rate was diminished, which mainly reduced the free heat of the reaction.

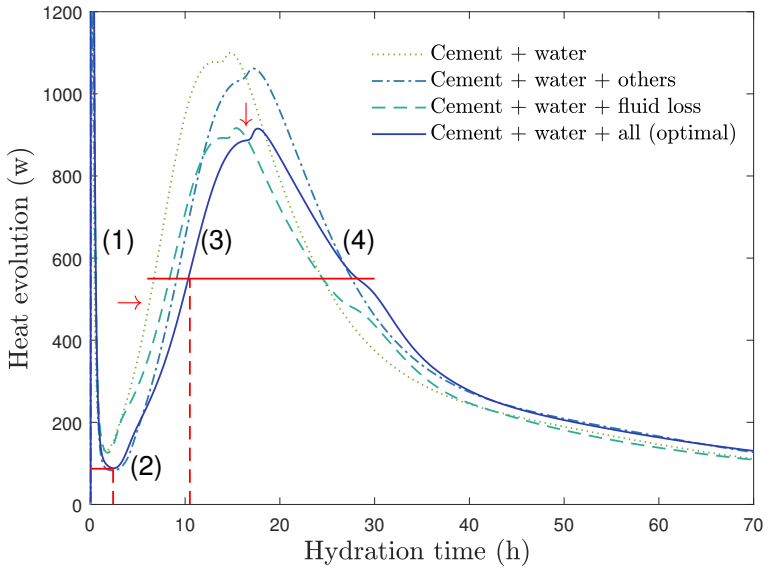


Figure 2: Rate of evolution heat of optimal cement paste. The red lines are the initial and approximately half the maximum of the main hydration peak. The right arrow indicates the dislocation of the main hydration peak with the addition of other additives (*retarder and defoamer*), and the down arrow shows the decrease of heat rate with the addition of *fluid loss* additive.

In the next section, we focus on characterizing the cement paste chosen by rheology and microscopy analysis of step (1) when the first stage of the hydration process happens.

### 3.2 Characterization of optimal cement paste

Figure 3a provides a detailed view of the isothermal calorimetry data captured during the initial three hours of hydration for the optimal cement paste (zoom of Fig. 2). By examining this specific period, we inferred the impact of the reactions and components involved in the initial stages of hydration on the resulting rheology (Fig. 3b) and microscopy (Fig. 3c) outcomes.

Drawing from existing literature, from this figure, we have identified the key factors contributing to the behavior of the heat generation rate during these initial three hours, which are as follows:

- The wetting of granules (1).

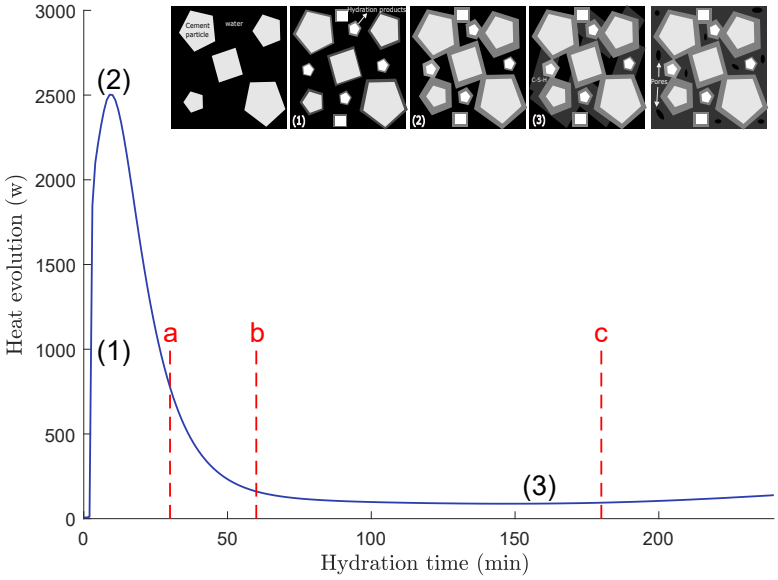


(a) Zoom of isotherm calorimetry (Figure 2).

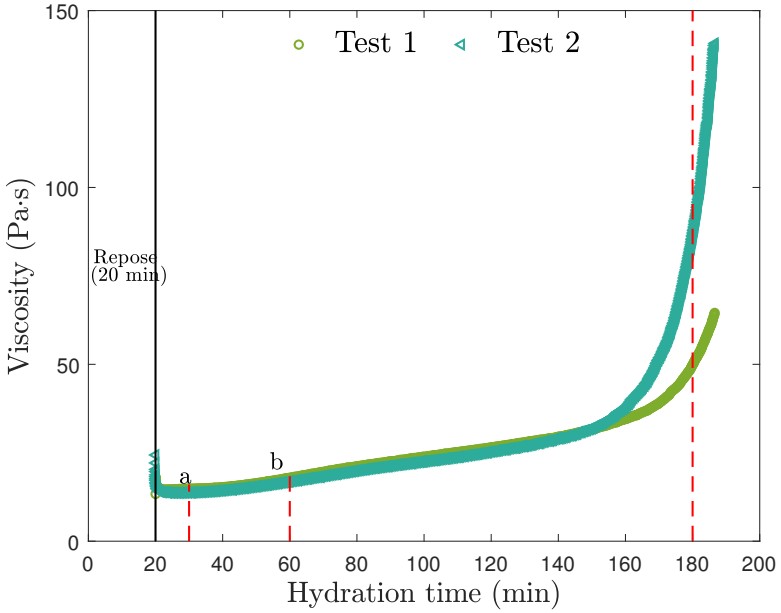


(b) Viscosity versus hydration time at a constant shear rate ($\dot{\gamma} = 1s^{-1}$)

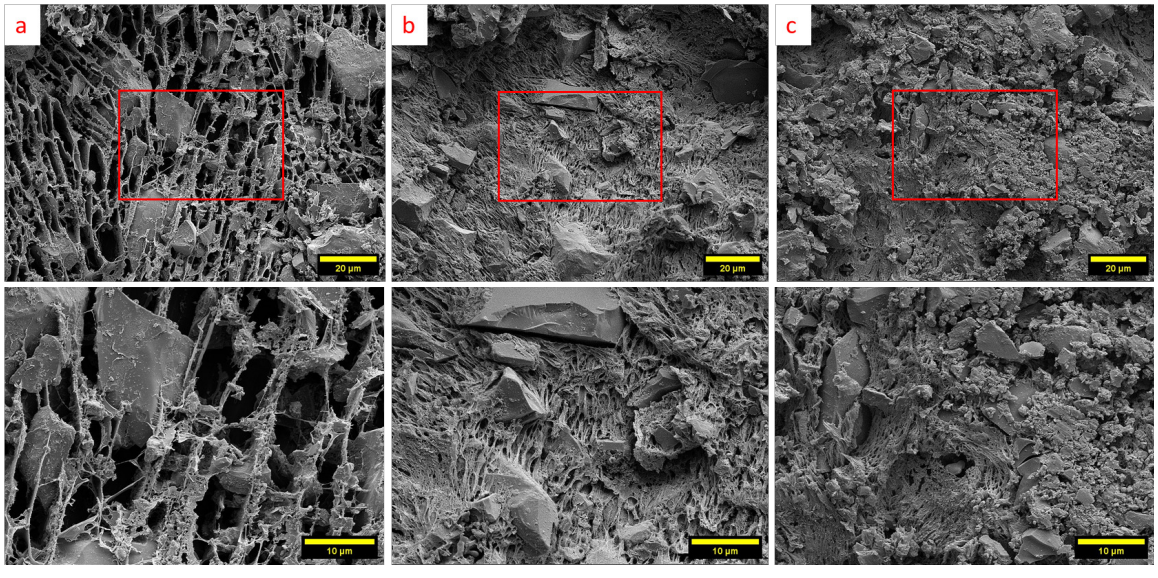


(c) Cryo-SEM micrographs (2000 and 5000x magnification)

Figure 3: Characterization of optimal cement paste. Red discontinuous lines from Fig. a) and b) represent the same points of hydration time in Cryo-SEM micrographs at 0.5 h, 1 h, and 3 h of hydration time..

- The fast dissolving of some mineral components (2).
- The precipitation of ettringite (2).
- Begining of induction period (3).

During the transition between stages (1) and (2), the rapid increase in heat generation is primarily attributed to the neutralizing electrostatic charges on the surface and the dissolution of calcium sulfate ($CaSO_4$) and alkali sulfates. Moreover, the dissolution of the C3S (alite) and C3A (calcium aluminate) phases liberates ions such as $K^+$, $Na^+$, $SO_4^{2-}$, and $Ca^{2+}$, which subsequently saturate the solution. Moving from stages (2) to (3), the consumed dissolved sulfate contributes to the formation of small, rigid needles of ettringite (AFt) and plates of monosulfoaluminate (AFm). Finally, during stage (3), there is a continuous development of the C-S-H network, characterized by the formation of calcium-silicate-hydrate (Ylmén *et al.* (2009)).

At the initial stage of the curve, a viscosity reduction is observed due to the time-dependent breakdown of the cement paste structure (de Miranda *et al.* (2023)). Subsequently, the viscosity remains relatively constant, representing a state of quasi-steady equilibrium (de Miranda *et al.* (2023)). Eventually, the viscosity experiences an exponential increase due to the formation of the calcium-silicate-hydrate (C-S-H) gel and various other reactions. The viscosity increment over time can be attributed to attractive particle forces, including van der Waals interactions and electrostatic forces, which are enhanced by the dissolution and precipitation of cement hydrates (Romano *et al.* (2018)). The enlargement of the cement-specific surface area is driven by the development of the C-S-H fibrillar network, as well as the formation of portlandite and ettringite (Aft) (Emri *et al.* (2014)). It is crucial to conclude the rheological tests before the solidification stage (stage 3) of the isothermal curve (refer to Fig. 2), which typically occurs after approximately three hours. Hence, any rheological measurements must be conducted during the induction phase (stage 2), wherein a quasi-equilibrium state exists between the ongoing reaction and the breakdown of the paste structure due to the shear rate applied.

The microstructure evolution of paste was observed by cryo-SEM at 30 min (a), one h (b), and three h (c), respectively. We prepared each test separately to ensure a comparable shear history. Figure 3c shows the interparticle network structure that progressively became denser as time elapsed, attributed to the precipitation and accumulation of reaction products on the network structure. The pore size decreased as gradually filled by the gel-like primary reaction products (C-S-H) (Liu (2014)).

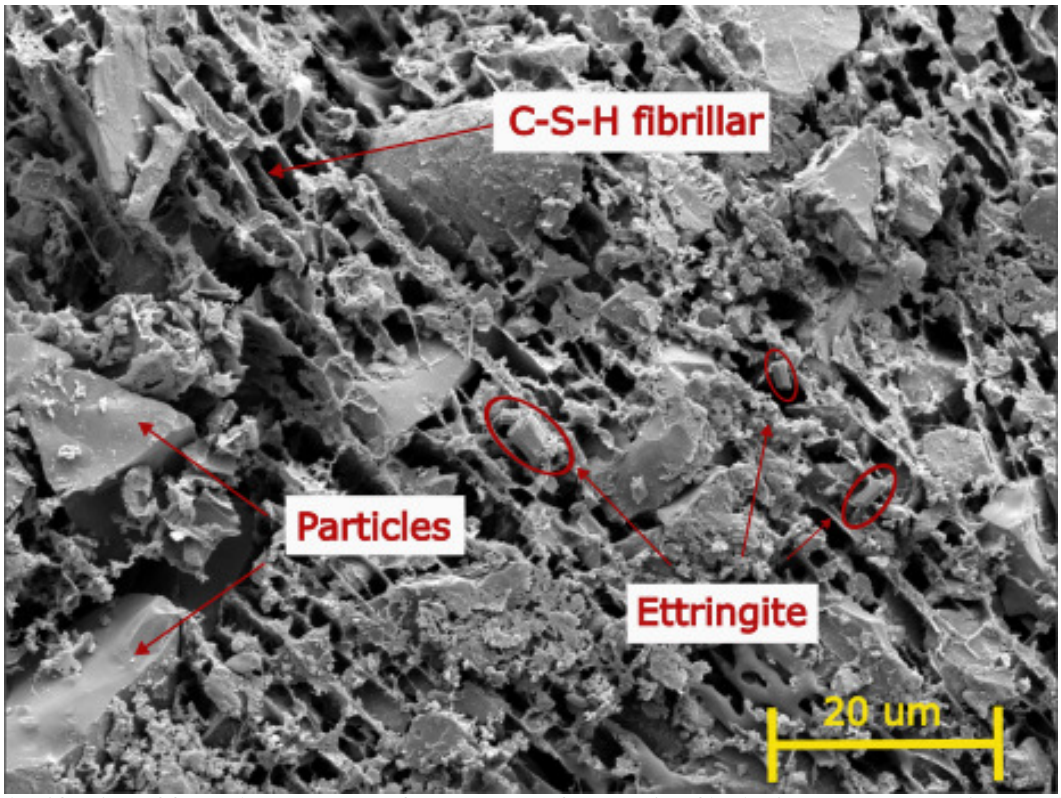

Figure 4: Identification of formed components of cement past after 30 min of hydration. Cryo-SEM micrograph at 3000x.

Figure 4 presents SEM micrographs of cement paste at the 30-minute hydration stage. In addition to large cement particles, two distinct hydration products can be observed (Fig. 4). Hexagonal and short-prismatic euhedral crystals, with lengths below 500 nm, are discernible, which aligns with the typical sizes reported in the literature for such crystals (Zingg

*et al.* (2008)). Based on their morphology, these crystals can be identified as ettringite. The second hydration component appears as fibrous and finer minerals, recognized as C–S–H. Hexagonal ettringite and fine fibers interconnect to form a network of hydration products interacting with clinker particles. Other researchers have reported similar findings (Zingg *et al.* (2008); Fylak *et al.* (2006); Kong *et al.* (2016)).

The development of these microstructures is influenced by various parameters, including the chemical composition of the cement and pore solution, types of hydrate phases, particle size distribution, and water-to-cement ratio (Zingg *et al.* (2008)). It is likely that these same parameters also exert a strong influence on the microstructure of fresh cement paste. This notion is supported by Fylak's study, which examined two different cement groups. The first group comprised ordinary Portland cement (OPCs), while the second group comprised two rapidly hardening cement (HSSC). The results revealed distinct ettringite morphologies for these two cement types. Needle-shaped ettringite was observed in one group (OPCs), whereas the other group (HSSC) exhibited ettringite with a short prismatic morphology, consistent with the observations in this study (Fylak *et al.* (2006)).

## 4. CONCLUSION

Initially, we developed a comprehensive methodology and optimized formulation to achieve a stable cement paste without water separation or sedimentation, ensuring consistent and reproducible results for rheological experiments. Subsequently, we employed calorimetry, rheology, and microscopy techniques to investigate the cement pastes' hydration process and microstructure development. These analyses were conducted in situ, allowing for continuous observation of the hydration process from the initial setting of the fresh pastes.

Each of the three techniques employed provided unique insights into different aspects of the cement paste hydration process. By correlating these aspects, we gain a more comprehensive understanding of the underlying phenomena. The chemical reactions occurring during hydration lead to the formation of hydrated compounds and a solid network that supports the cement particles, resulting in the evolution of the material's physical properties over time. Increased viscosity and rigidity accompany this transition from a fluid to a solid state. We better undestand that the rheology experiments must be limited to the induction stage (2) (refer to Fig. 2), which represents a quasi-stable period characterized by a quasi-equilibrium between the ongoing reactions and the breakdown of the paste structure.

## 5. ACKNOWLEDGEMENTS

The authors thank Petrobras S. A. (2017/00426-9), ANP(PRH-01.19.0248.00), 200 CNPq(307976/2018-1), CAPES (PROEX 625/2018), and FAPERJ(E-26/202.834/2017) 201 for the financial support to the Rheology Group at PUC-Rio.

## 6. REFERENCES

Baudez, J.C., Chabot, F. and Coussot, P., 2002. "Rheological interpretation of the slump test". *Applied Rheology*, Vol. 12, No. 3, pp. 133–141.

de Miranda, L.R., Marchesini, F.H., Lesage, K. and De Schutter, G., 2023. "The evolution of the rheological behavior of hydrating cement systems: Combining constitutive modeling with rheometry, calorimetry and mechanical analyses". *Cement and Concrete Research*, Vol. 164, p. 107046.

Emri, I., Gonzalez-Gutierrez, J., Gergesova, M., Zupancic, B. and Saprunov, I., 2014. "Experimental determination of material time-dependent properties". *Encyclopedia of Thermal Stresses*, pp. 1494–1510.

Fylak, M., Goske, J., Kachler, W., Wenda, R. and Pollmann, H., 2006. "Cryotransfer scanning electron microscopy for the study of cementitious systems". *Microscopy and Analysis*, Vol. 114, p. 9.

ISO, B. *et al.*, ???? "Petroleum and natural gas industries, cements and materials for well cementing, specification". *BS EN ISO*, pp. 10426–1.

Kong, X., Pakusch, J., Jansen, D., Emmerling, S., Neubauer, J. and Goetz-Neuhoeffer, F., 2016. "Effect of polymer latexes with cleaned serum on the phase development of hydrating cement pastes". *Cement and Concrete Research*, Vol. 84, pp. 30–40.

Liu, F., 2014. "Early-age hydration studies of portland cement".

M. Fylak, J. Göske1, W.K.R.W.H.P., 2006. "Cryotransfer scanning electron microscopy for the study of cementitious systems". *Microscopy and analysis*, Vol. 102, No. 6, pp. 9–12.

Mangadlao, J.D., Cao, P. and Advincula, R.C., 2015. "Smart cements and cement additives for oil and gas operations". *Journal of Petroleum Science and Engineering*, Vol. 129, pp. 63–76.

Nelson, E.B., 1990. *Well cementing*. Newnes.

Peng, Y., Lauten, R.A., Reknes, K. and Jacobsen, S., 2017. "Bleeding and sedimentation of cement paste measured by hydrostatic pressure and turbiscan". *Cement and Concrete Composites*, Vol. 76, pp. 25–38.

Rodrigues, E.C. and de Souza Mendes, P.R., 2019. "Predicting the time-dependent irreversible rheological behavior of oil well cement slurries". *Journal of Petroleum Science and Engineering*, Vol. 178, pp. 805–813.

Romano, R.C.d.O., Cincotto, M.A. and Pileggi, R.G., 2018. "Hardening phenomenon of portland cement suspensions monitored by vicat test, isothermal calorimetry and oscillatory rheometry". *Revista IBRACON de Estruturas e Materiais*, Vol. 11, pp. 949–959.

Roussel, N. and Coussot, P., 2005. ""fifty-cent rheometer" for yield stress measurements: from slump to spreading flow". *Journal of rheology*, Vol. 49, No. 3, pp. 705–718.

Roussel, N., Stéfani, C. and Leroy, R., 2005. "From mini-cone test to abrams cone test: measurement of cement-based materials yield stress using slump tests". *Cement and concrete research*, Vol. 35, No. 5, pp. 817–822.

Shahriar, A., 2011. *Investigation on rheology of oil well cement slurries*. The University of Western Ontario (Canada).

Sun, Y., Zhang, S., Rahul, A., Tao, Y., Van Bockstaele, F., Dewettinck, K., Ye, G. and De Schutter, G., 2022. "Rheology of alkali-activated slag pastes: New insight from microstructural investigations by cryo-sem". *Cement and Concrete Research*, Vol. 157, p. 106806.

Talevi, R., Barbato, V., Fiorentino, I., Braun, S., De Stefano, C., Ferraro, R., Sudhakaran, S. and Gualtieri, R., 2016. "Successful slush nitrogen vitrification of human ovarian tissue". *Fertility and Sterility*, Vol. 105, No. 6, pp. 1523–1531.

Ylmén, R., Jäglid, U., Steenari, B.M. and Panas, I., 2009. "Early hydration and setting of portland cement monitored by ir, sem and vicat techniques". *Cement and Concrete Research*, Vol. 39, No. 5, pp. 433–439.

Zingg, A., Holzer, L., Kaech, A., Winnefeld, F., Pakusch, J., Becker, S. and Gauckler, L., 2008. "The microstructure of dispersed and non-dispersed fresh cement pastes—new insight by cryo-microscopy". *Cement and Concrete Research*, Vol. 38, No. 4, pp. 522–529.

## 7. RESPONSIBILITY NOTICE

The authors are solely responsible for the printed material included in this paper.